ELSEVIER

Solid State Ionics 76 (1995) 91–96

SOLID STATE IONICS

Diffusion enhancement in $Li_xMn_2O_4$

Liquan Chen *, Xuejie Huang, Erik Kelder, Joop Schoonman

Laboratory for Inorganic Chemistry, Delft University of Technology, P.O. Box 5045, 2600 GA Delft, The Netherlands

Received 6 June 1994; accepted for publication 7 October 1994

Abstract

The electrochemical properties of $Li_xMn_2O_4$ with $0.5 \leq x \leq 2.5$ as the lithium content in the starting materials, have been studied. A novel wet-chemical route has been developed. The lithium chemical diffusion coefficient in $Li_xMn_2O_4$ as synthesized by this wet-chemical technique is at least 10 times higher than that of $LiMn_2O_4$ obtained by solid state reaction. In the observed two-phase regions near $x=0.75$ and 1.75 diffusion enhancement ascribed to interfacial diffusion is observed. The results of cyclic voltammetry and impedance analysis provide additional evidence for this hypothesis.

Keywords: Lithium battery; Manganese oxide; Lithium manganese oxide

1. Introduction

Rechargeable lithium batteries are currently of great interest and some are being commercialized by Moli Energy Ltd. and Sony Energy Inc. [1–3]. The cathode materials used in these batteries are $LiNiO_2$ or $LiCoO_2$. Among the candidate cathode materials reported to date $LiMn_2O_4$ with spinel structure has been studied extensively. The rechargeable capacity of $LiMn_2O_4$ is 100–130 mAh/g which is comparable to that of $LiCoO_2$ [4]. $LiMn_2O_4$ is easy to prepare and less expensive than $LiCoO_2$ and $LiNiO_2$. Therefore, the overall cost of the battery would be reduced if $LiMn_2O_4$ is used as cathode material.

Usually $LiMn_2O_4$ is prepared by solid state reaction in air. It can be formed between 200 and 1000°C. The influence of the calcining temperature on the properties of $LiMn_2O_4$ has been investigated [5,6]. The material calcined at 450°C contains Mn_2O_3. With increasing of the calcining temperature, the amount of impurity phase decreases, and more pure $LiMn_2O_4$ with less defects could be obtained. However, the chemical diffusion coefficient in samples calcined at lower temperature is obviously higher than that in samples calcined at higher temperature. For instance, $\tilde{D}=4.9\times10^{-9}$ cm^2/s in samples calcined at 450°C, while $\tilde{D}$ is 6.0×10^{-10} cm^2/s in a sample calcined at 1100°C [6]. This difference may be attributed to variations in defect and microstructure, or residual strain of the $LiMn_2O_4$ powder. It has been proven that cathodes made from powders with smaller particle size posses better reversibility, smaller polarization, and higher capacity [5].

In order to obtain submicron powders and a lower synthesis temperature, a wet-chemical technique has been developed. The use of acetates as precursors for the low-temperature synthesis of $LiMn_2O_4$ has been reported in some detail, i.e. such as the role of the starting materials and the ambient atmosphere, as well as the dependence of thermal reactivity of an acetate xerogel on the Li/Mn ratio [7].

* On leave from Institute of Physics, Academia Sinica, P.O. Box 603, Beijing 100080, China.

SSDI 0167-2738(94)00223-1

In the present paper the electrochemical properties of $Li_xMn_2O_4$ synthesized by this new wet-chemical technique are reported. The emphasis will be on the relation between an observed diffusion enhancement and the nominal compositions of $Li_xMn_2O_4$.

2. Experimental

The powder samples have been synthesized by using an aqueous solution of lithium hydroxide and manganous acetate with various Li/Mn ratios. For simplicity a nominal formula $Li_xMn_2O_4$ is used hereafter for the synthesized products. The x value represents the lithium molar content in the starting material. The deposits were calcined at 600°C for 10 h. The details of the synthesis procedure and the characterization will be reported in a forthcoming paper [8].

All the $Li_xMn_2O_4$ powders were heated at 150°C for 24 h prior to being used as an electrode in order to eliminate any possibility of water contamination. The products were identified by a PW 1840 compact powder diffractometer (Philips) using CuKα radiation at a scan rate of 0.5°/min.

The electrochemical properties of $Li_xMn_2O_4$ were investigated by using the galvanic cell:

$$Li/1\ M\ LiAsF_6 \quad in \quad PC+DME/Li_xMn_2O_4,$$

which consists of a lithium foil anode, a piece of nonwoven polypropylene cloth soaked in PC+DME (1:1) with 1 M $LiAsF_6$ as electrolyte, and $Li_xMn_2O_4$ as the cathode. Thin film cathodes were made of $Li_xMn_2O_4$ and 3 wt% teflon powder as binder without any other conductive additives.

The chemical diffusion coefficients of Li^+ ions in $Li_xMn_2O_4$ were measured at room temperature by the Galvanostatic Intermittent Titration Technique (GITT) [9] using a Galvanostatic/Potentiostatic System, Model 273, Princeton Applied Research. When the voltage variation was less than 5 mV per day, the value was defined as the equilibrium value.

The cyclic voltammogram of the same cell was obtained between 2.5 and 4.3 V using the same Galvanostatic/Potentiostatic System combined with an X–Y recorder BP 90. The scan rate was choosen to be 1 mV/s.

The impedance spectra of the cells were measured using a Solatron 1255 Frequency Response Analyzer in conjunction with a Solatron 1286 Electrochemical Interface. The impedance data were measured at the equilibrium potential, i.e. under conditions of absence of a dc current flow, which was achieved by first measuring the open-circuit voltage (OCV) of a cell, compensating this value with the electrochemical interface, and subsequently waiting for a certain time until the current through the cell is very small. The amplitude of the ac signal is 20 mV. The impedance data were analyzed using a non-linear least-squares computer fit program developed by Boukamp [10].

3. Results and discussion

3.1. Lithium diffusion enhancement

The chemical diffusion coefficients of Li^+ in $Li_xMn_2O_4$ are presented in Fig. 1a as a function of the nominal composition x at room temperature. Two important features should be noted.

Firstly, the lithium diffusion is enhanced in all nominal compositions studied. The chemical diffusion coefficient in $LiMn_2O_4$ calcined at 450°C by solid state reaction is 4.9×10^{-9} cm^2/s [6], while the values in Fig. 1a range from 3.3×10^{-8} to 7.7×10^{-7} cm^2/s. At least one order of magnitude higher chemical diffusion coefficients are observed. In samples calcined at 300°C, the primary particle size varies from 0.03 to 1 μm, while the primary particle size of samples calcined at 800°C ranges from 0.1 to 3 μm [7]. In spite of the variations in primary particle size, the chemical diffusion coefficient is nearly in the same order of magnitude, i.e. about 10^{-9} cm^2/s [6,11]. The primary particle size of the present samples is measured to be about 1 μm by SEM. If the diffusion is influenced by grain boundaries it may be concluded that in the samples calcined at different temperatures total grain boundary surfaces are comparable. The diffusion enhancement in the present samples, in which the grain boundary surface area seems to be of comparable magnitude, should then be related with defects, compositional inhomogeneities at the grain boundaries, or with highly conductive interfacial regions between conducting, and poorly conducting phases.

Secondly, two maxima of $\tilde{D}$ in the curve $\tilde{D}$ versus

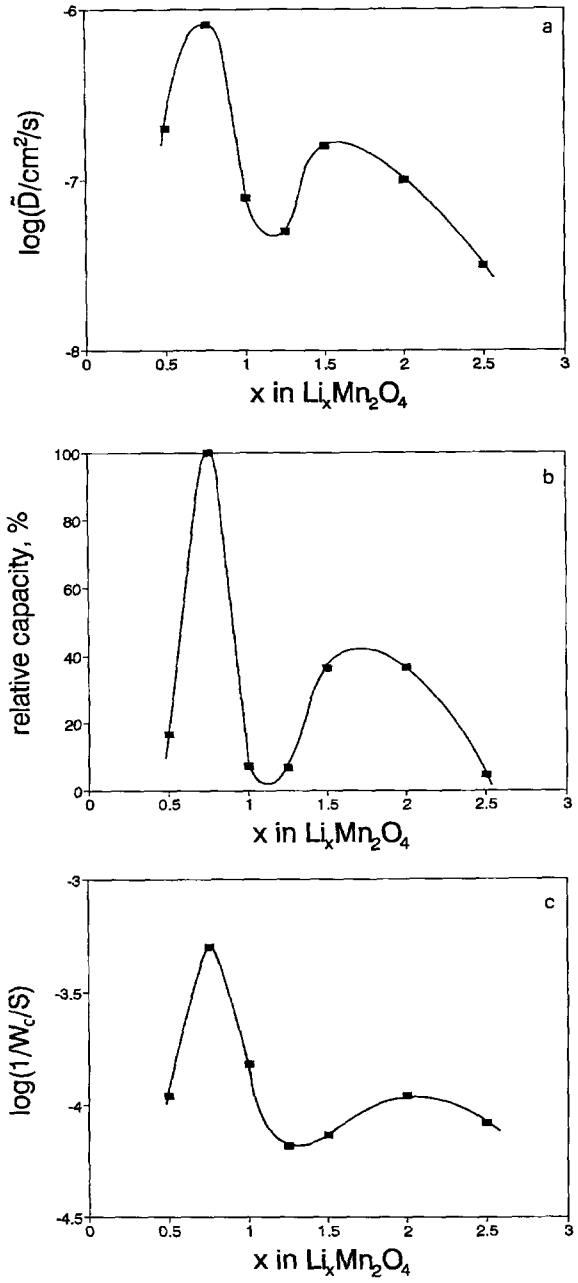

Fig. 1. Several electrochemical parameters of the present $Li_xMn_2O_4$ phases as a function of the nominal composition x: (a) Chemical diffusion coefficient; (b) relative capacity as obtained from cyclic voltammograms; (c) inverse constant of the Warburg impedance.

x clearly appear near the values 0.75 and 1.75 for x, respectively. These maxima are ascribed to diffusion enhancement resulting from interfacial defects formed between the principal phase $LiMn_2O_4$ and dispersed second phase particles (DSPP) comprising Mn_2O_3 or Li_2MnO_3. It can be seen from XRD patterns in Fig. 2 that the single spinel phase $LiMn_2O_4$ was obtained for x is 1.25. The impurity phase Li_2MnO_3 is formed, and the amount increased gradually with increasing amounts of Li in the starting materials. As a result, the colour of the products turns to orange. On the other hand, the peaks of the impurity phase Mn_2O_3 are observed in XRD patterns of $Li_xMn_2O_4$ with decreasing of amounts of Li. Both Li_2MnO_3 and Mn_2O_3 are not suitable as cathode materials in rechargeable lithium batteries due to their poor dischargeability [12]. Since they were formed as co-deposits in addition to $LiMn_2O_4$, they were highly dispersed into the host matrix. This situation is comparable to that of composite ionic conductors, comprising two-phase mixtures of an ionic conductor and an inert oxide with high surface area [13–15]. Such composites exhibit enhanced ionic conductivity. Even two orders of magnitude enhancement of the ionic conductivity in LiX (Al_2O_3) (X = halides) has been observed. The mechanism of this enhancement is suggested to be the formation of highly conductive interfacial regions between particles of the two phases. The maximum conductivity appears at about 25 mol% of the inert second phase in the composite ionic conductors. The maximum diffusion enhancement in the present case is ob-

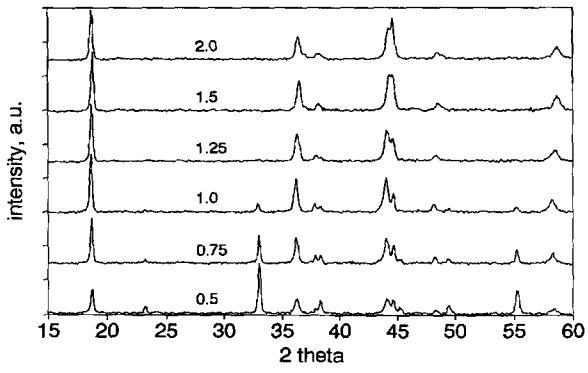

Fig. 2. X-ray diffraction patterns of $Li_xMn_2O_4$ powders synthesized by the wet-chemical method, and calcined at 600°C for 10 h.

served near the same amount of the second phase i.e. Mn_2O_3 or Li_2MnO_3. In the pure spinel phase of $LiMn_2O_4$, synthesized by the described wet-chemical technique, the chemical diffusion coefficient is found in the range 4.7 to 7.9×10^{-8} cm^2/s. With the addition of the second phase the diffusion coefficient increases and reaches a maximum near $x=0.75$ and $x=1.75$. At still higher second phase amounts the bulk diffusion of the second phase becomes predominant, and, therefore, the diffusion coefficient decreases.

It should be noted that the maximum of D near $x=0.75$ is much higher than that near $x=1.75$. Another factor affecting the diffusion may be the formation of nonstoichiometric $Li_{1-x}Mn_2O_4$. The unit cell parameter for $Li_{1-x}Mn_2O_4$ is 8.067 Å, while the value for $LiMn_2O_4$ is 8.24762 Å [16,17]. By comparing the XRD peak (511) or (333) for samples with various lithium content in starting materials, it can be noticed that 2θ shifts towards lower angles when x increases from 0.5 to 1.0 and then remains constant for $x=1.0$ to 1.25. This indicates that the formation of nonstoichiometric $Li_{1-x}Mn_2O_4$ near $x=0.75$. The lithium diffusion in $Li_{1-x}Mn_2O_4$ may be facilitated by the larger channels in the structure.

A further discussion of the diffusion enhancement will be presented in the next sections.

3.2. Cyclic voltammograms

Some typical cyclic voltammograms of the present cells are shown in Fig. 3. In all cases the reversibility is rather good. For a two-electrode system it is usually not easy to observe the intercalation and de-intercalation peaks. In Fig. 3, except for the cell with the $Li_{1.25}Mn_2O_4$ cathode material, the lithium intercalation and de-intercalation peaks can be distinguished clearly. It can be seen that the voltage separation between the peaks in the oxidation scan and in the reduction scan is lower for $x=0.75$. This implies that the cathode with $x=0.75$ has the smallest polarization, because it has the highest chemical diffusion coefficient as mentioned above.

The area covered by the cyclic voltammogram represents the capacity of a cell during an oxidation and reduction cycle, because the Y-axis represents the current flowing through the cell and the X-axis is in fact a time interval of the cycle. The relative capacities of the cell with different nominal compositions

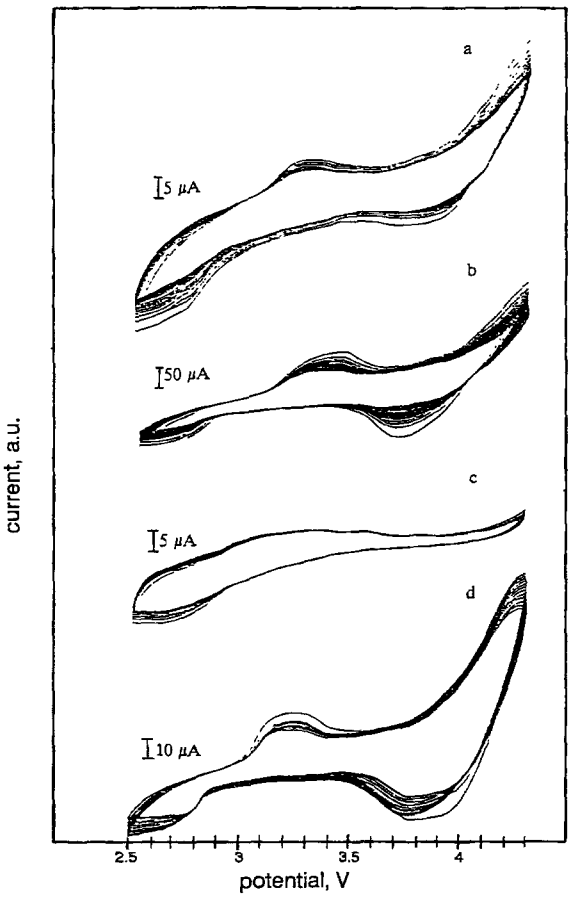

Fig. 3. Cyclic voltammograms of the cell Li/1 M $LiAsF_6$ in PC+DME/$Li_xMn_2O_4$ between 2.5 V and 4.3 V at a scanning rate of 1 mV/s: (a) $x=0.5$, (b) $x=0.75$, (c) $x=1.25$ and (d) $x=1.5$.

$Li_xMn_2O_4$ as a cathode material are shown in Fig. 1b. This curve is very similar to the curve of $\tilde{D}$ versus x. Two maxima appear at the same x values as in Fig. 1a. This shape of the curve is understandable by considering diffusion enhancement in the $Li_xMn_2O_4$ cathodes near $x=0.75$ and 1.75. Some other factors such as the electrolyte resistance, the interfaces between the electrolyte, the anode as well as the cathode will also influence the cell capacity. The following impedance analysis will show that the capacity maxima are mainly caused by enhanced diffusion in the $Li_xMn_2O_4$ cathode.

3.3. Impedance analysis

Fig. 4a–d shows the impedance spectra of cells with $Li_xMn_2O_4$ as cathode for $x=0.5$, 0.75, 1.25 and 1.5, respectively.

The impedance of each electrode of a cell comprises double layer capacitances, charge transfer resistances and a Warburg impedance. The Warburg impedance is connected with the cathode. The electrolyte will contribute a resistance to the battery impedance. A simplified equivalent circuit for the battery, as shown in Fig. 4e, was used to fit the experimental data. Fig. 4a–d shows the NLLS fit data compared with the experimental impedance spectra. The fit results for the impedance spectra are listed in Table 1. It can been seen from Table 1 that the cell with the $Li_{0.75}Mn_2O_4$ cathode has the highest R, R_a and R_c. Therefore, the relative capacity is only induced by the enhanced diffusion coefficient.

The plot of inverse Warburg impedance versus x is

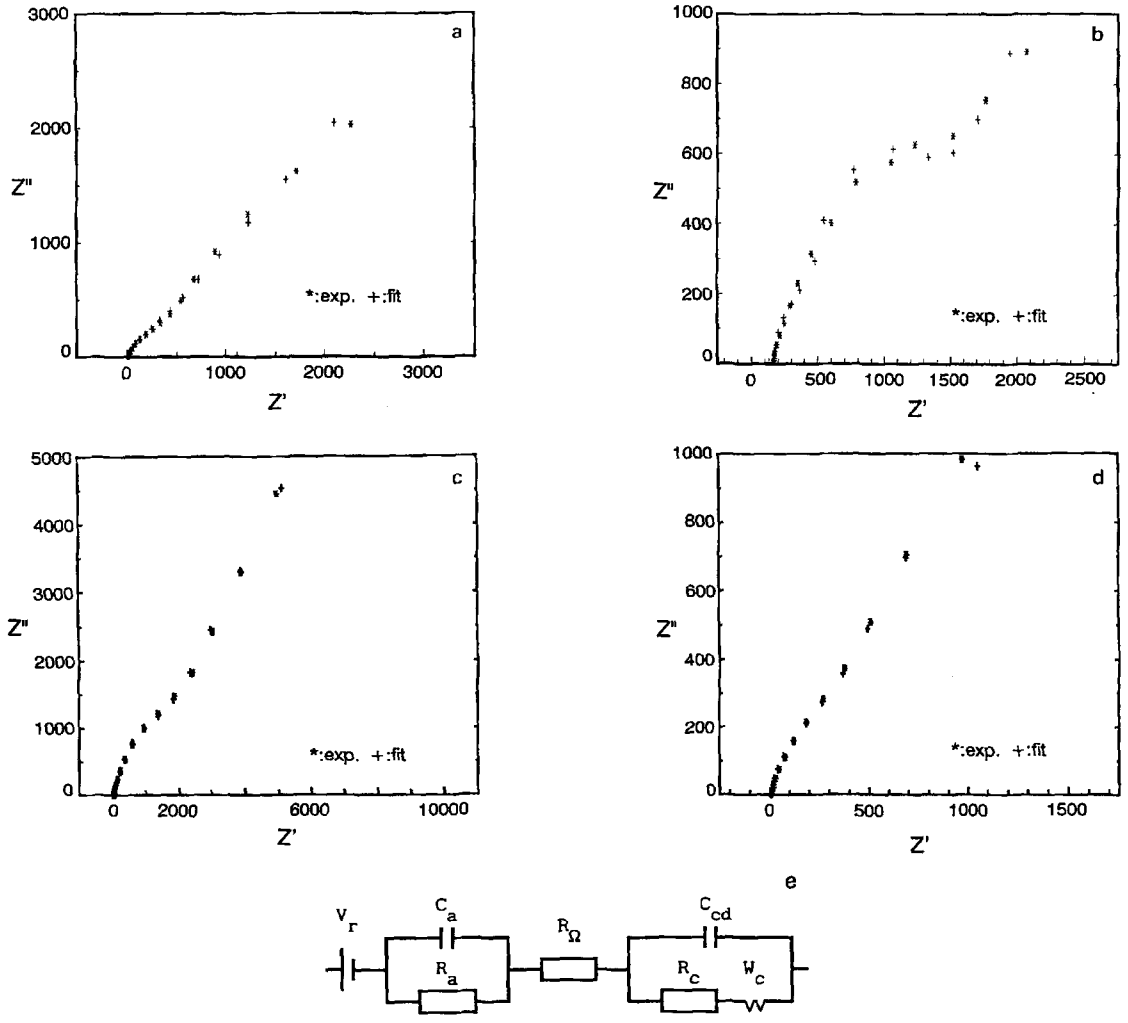

Fig. 4. Impedance spectra and NLLS fit results of cells with $Li_xMn_2O_4$ as cathode: (a) $x=0.5$; (b) $x=0.75$; (c) $x=1.25$; (d) $x=1.5$ and (e) a simplified equivalent circuit of the cell. R=resistance of the electrolyte; C_{ad}, C_{cd}=double layer capacitances between anode or cathode and electrolyte, respectively. R_a, R_c=charge transfer resistances of anode and cathode, respectively. W_c=Warburg impedance of the cathode. V_r=Externally applied voltage to compensate the open circuit voltage of the cell.

Table 1
NLLS fit results for the impedance spectra of cells with $Li_xMn_2O_4$ as a cathode. The symbols are defined in the caption of Fig. 4

x	R (Ω)	C_{ad} (μF)	R_a (Ω)	C_{cd} (μF)	R_c (Ω)	$1/W$ (S)
0.5	12.4	1.78	14.2	1.16	139	1.09E−4
0.75	169	26.9	761	3.46	197	4.99E−4
1.0	7.57	72.2	316	0.674	87.4	1.52E−4
1.25	13.2	5.79	576	0.573	46.9	6.61E−5
1.5	6.12	1.15	2740	14.8	997	7.48E−5
2.0	11.38	0.823	1150	61.5	3180	1.1E−4
2.5	27.0	1.19	2.50	1.06	217	8.4E−5

given in Fig. 1c. Once again the curve has the same shape as that of $\tilde{D}$ versus x, which means two maxima are observed near $x=0.75$ and 1.75. The cell with $x=0.75$ has the lowest Warburg impedance. Qualitatively the Warburg prefactor is inversely proportional to the chemical diffusion coefficient. The impedance analysis results provide additional evidence of the diffusion enhancement in certain nominal composition ranges for the $Li_xMn_2O_4$ cathodes synthesized by the present wet-chemical technique.

Due to the observed enhancement of the ionic conductivity resulting from the two-phase systems of $LiMn_2O_4+Mn_2O_3$ and $Li_xMn_2O_4+Li_2MnO_3$ [#] it is claimed to improve the capacity of the battery as a whole, by mixing submicron powders of Mn_2O_3 and $Li_xMn_2O_4$ $(1.0<x<1.5)$, or mixtures of $Mn_2O_3+LiMn_2O_4$ and $Li_xMn_2O_4$ $(1.0<x<1.5)$, eventually synthesized by the wet-chemical method described above. In addition, mixtures of $Li_xMn_2O_4$ $(1.0<x<1.5)$ and submicron alumina (Al_2O_3) could also be promising, with respect to high Li^+ ionic conductivity. This option is currently being studied.

4. Conclusions

The spinel phase $LiMn_2O_4$ synthesized by a new wet-chemical technique exhibits at least a 10 times higher diffusion coefficient compared with that obtained by a solid state reaction. In addition, an interfacial diffusion enhancement has been observed in two two-phase regions near $x=0.75$ and $x=1.75$. The two-phase regions are $LiMn_2O_4+Mn_2O_3$ and $Li_xMn_2O_4+Li_2MnO_3$ [#]. The cathodes with these nominal composition showed improved reversibility, higher capacity, and lower Warburg impedance.

[#] Here x is an unknown but distinct value.

References

[1] J.R. Dahn, U. Von Stacken and R. Fong, The Electrochemical Society Extended Abstracts, Vol 90–2 (Seattle, WA, October 14–19, 1990) Abstract 42, p. 66.
[2] T. Nagaura, 4th Intern. Rechargeable Battery Seminar, Deerfield Beach, Florida (1990).
[3] T. Nishi, H. Azuma and A. Omaru, U.S. Patent 4,959,281 (1990).
[4] T. Ohzuku, A. Ueda and M. Nagayama, J. Electrochem. Soc. 140 (1993) 1862.
[5] J.M. Tarascon, E. Wang, F.K. Shokoohi, W.R. McKinnon and S. Colson, J. Electrochem. Soc. 138 (1991) 2859.
[6] L. Chen and J. Schoonman, 67 (1993) 17.
[7] P. Barboux, J.M. Tarascon and F.K. Shokoohi, J. Solid State Chem. 94 (1990) 185.
[8] E.M. Kelder, L. Chen and J. Schoonman, Solid State Ionics, submitted for publication.
[9] W. Weppner and R.A. Huggins, J. Electrochem. Soc. 124 (1977) 1569.
[10] B.A. Boukamp, Internal Report, CT 89/214/128.
[11] D. Guyomard and J.M. Tarascon, J. Electrochem. Soc. 139 (1992) 937.
[12] T. Nohma, T. Saito, N. Furukawa and H. Ikeda, J. Power Sources 26 (1989) 389.
[13] C.C. Liang and L.H. Barnette, J. Electrochem. Soc. 123 (1976) 453.
[14] G. Wang, Z.R. Li, L.Q. Chen, and Z.Y. Zhao, Acta Phys. Sinica 30 (1981) 1569.
[15] L. Chen, L.Z. Wang, G. Che, G. Wang, and Z. Li, Solid State Ionics 14 (1984) 149.
[16] Natl. Bur. Stand. (U.S.) Monogr. 25, 2178 (1984).
[17] M. Thackeray, P.J. Johnson, L.A. De Picciotto, P.G. Bruce and J.B. Goodenough, Mater. Res. Bull. 19 (1984) 179.